Photocycle of Halorhodopsin from *Halobacterium salinarium*

György Váró,* László Zimányi,* Xiaolei Fan,‡ Li Sun,‡ Richard Needleman,‡ and Janos K. Lanyi*
*Department of Physiology and Biophysics, University of California, Irvine, Irvine, California 92717, and ‡Department of Biochemistry, Wayne State University School of Medicine, Detroit, Michigan 48201 USA

ABSTRACT The light-driven chloride pump, halorhodopsin, is a mixture containing all-*trans* and 13-*cis* retinal chromophores under both light and dark-adapted conditions and can exist in chloride-free and chloride-binding forms. To describe the photochemical cycle of the all-*trans*, chloride-binding state that is associated with the transport, and thereby initiate study of the chloride translocation mechanism, one must first dissect the contributions of these species to the measured spectral changes. We resolved the multiple photochemical reactions by determining flash-induced difference spectra and photocycle kinetics in halorhodopsin-containing membranes prepared from *Halobacterium salinarium*, with light- and dark-adapted samples at various chloride concentrations. The high expression of cloned halorhodopsin made it possible to do these measurements with unfractionated cell envelope membranes in which the chromophore is photostable not only in the presence of NaCl but also in the Na_2SO_4 solution used for reference. Careful examination of the flash-induced changes at selected wavelengths allowed separating the spectral changes into components and assigning them to the individual photocycles. According to the results, a substantial revision of the photocycle model for *H. salinarium* halorhodopsin, and its dependence on chloride, is required. The cycle of the all-*trans* chloride-binding form is described by the scheme, $HR\text{-}^{h\nu} \rightarrow K \Leftrightarrow L_1 \Leftrightarrow L_2 \Leftrightarrow N \rightarrow HR$, where HR, K, L, and N designate halorhodopsin and its photointermediates. Unlike the earlier models, this is very similar to the photoreaction of bacteriorhodopsin when deprotonation of the Schiff base is prevented (e.g., at low pH or in the D85N mutant). Also unlike in the earlier models, no step in this photocycle was noticeably affected when the chloride concentration was varied between 20 mM and 2 M in an attempt to identify a chloride-binding reaction.

INTRODUCTION

The halorhodopsins are small retinal proteins in the cytoplasmic membrane of halobacteria (Lanyi, 1986b, 1990; Oesterhelt et al., 1992). The amino acid sequence of the different variants from various halobacterial species (Blanck and Oesterhelt, 1987; Lanyi et al., 1990a; Otomo et al., 1992) and the overall three-dimensional structure of the *Halobacterium salinarium* halorhodopsin (Havelka et al., 1993) bear great similarity to the proton pump, bacteriorhodopsin. As in the other retinal protein, illumination causes isomerization of the retinal chromophore from all-*trans*, 15-*anti* to 13-*cis*, 15-*anti*, but the ensuing sequence of thermal reactions, evidenced by changes in its absorbance in the visible and the infrared (the photocycle), are accompanied by the inward translocation of a chloride ion (Schobert and Lanyi, 1982) rather than the outward transport of a proton. Thus, halorhodopsin functions as a light-driven electrogenic pump for chloride ions.

Lack of an aspartate residue equivalent to D85, the proton acceptor to the retinal Schiff base in bacteriorhodopsin, is consistent with the fact that under physiological conditions photoexcitation of halorhodopsin does not lead to deprotonation of the Schiff base. The intermediate states in this photocycle reflect instead only the changing configurational states of the retinal (Maeda et al., 1985; Diller et al., 1987; Rothschild et al., 1988; Ames et al., 1992), the transient binding of chloride to an arginine residue (Braiman et al., 1994; Walter and Braiman, 1994), and probably the changing influence of the protein on the chromophore as a chloride ion is moved from one membrane surface to the other. To understand how the chloride is transported, one must describe these light-initiated changes and understand their origins. There have been numerous attempts to describe the photocycle of halorhodopsin from *H. salinarium* (Tsuda et al., 1982; Hazemoto et al., 1983; Bogomolni, 1984; Hegemann et al., 1985; Oesterhelt et al., 1985; Lanyi and Vodyanoy, 1986; Tittor et al., 1987; Rothschild et al., 1988; Zimányi et al., 1989a; Zimányi and Lanyi, 1989a; Spencer and Dewey, 1990; Ames et al., 1992), and it appeared that in the presence of chloride it contained intermediate states more or less equivalent in their absorption spectra in the visible and the infrared and in the sequence of their rise and decay to K (or KL), L, and O of the bacteriorhodopsin photocycle. They were termed, respectively HR_K (HR_{KL}) or HR_{600}, HR_L or HR_{520}, and HR_O or HR_{640}. Many of the details of the halorhodopsin photocycle have been unclear or contradictory, however. In one report, the rise of the HR_{520} state was chloride dependent, suggesting that its formation depends on chloride binding (Tittor et al., 1987), but another study did not find such an effect (Zimányi and Lanyi, 1989a). The amplitudes of HR_{520} (HR_L) and HR_{640} (HR_O) varied reciprocally with chloride concentration in a way that suggested a chloride-dependent back-reaction in an $HR_L \Leftrightarrow HR_O$ equilibrium (Oesterhelt et al., 1985; Lanyi and Vodyanoy, 1986;

Received for publication 17 November 1994 and in final form 18 February 1995.

Address reprint requests to Dr. Janos K. Lanyi, Department of Physiology and Biophysics, University of California, Irvine, Irvine, CA 92717. Tel.: 714-824-7150; Fax: 714-824-8540; E-mail: lbrown2@orion.oac.uci.edu.

Permanent address of G. Váró and present address of L. Zimányi: Institute of Biophysics, Biological Research Center of the Hungarian Academy of Sciences, H-6701 Szeged, Hungary.

0006-3495/95/05/2062/11 $2.00

Tittor et al., 1987; Zimányi and Lanyi, 1989a; Ames et al., 1992). This would indicate release of chloride in the forward reaction, i.e., at the HR_L to HR_O step of the photocycle. However, the intermediates that arose thermally upon warming illuminated halorhodopsin from cryogenic temperatures did not include the HR_O state (Zimányi and Lanyi, 1989b). Finally, the rate constant of the decay of HR_O to the initial HR state was reported to increase with chloride concentration in one study (Ames et al., 1992) but not in the others.

Given the fact that this is a transport system for chloride, it was expected that the photochemical reaction cycle would be different in the absence of chloride. Maintaining constant ionic strength would have been best with sulfate, an apparently noninteracting anion (Ogurusu et al., 1982; Schobert and Lanyi, 1986), but the purified and detergent-solubilized chromophore was photolabile under these conditions. Nitrate was less effective in eliciting the chloride-type photocycle, consistent with the poorer transport of this anion (Zimányi and Lanyi, 1989a; Duschl et al., 1990), and it was used instead as the reference to the experiments with chloride. Indeed, in nitrate solutions of low concentration, an abbreviated cycle different from that in chloride was found, containing only a K (or KL) and an O-like state (Lanyi and Vodyanoy, 1986; Tittor et al., 1987; Zimányi and Lanyi, 1989a).

Describing the halorhodopsin photocycle is made very difficult by the fact that, like monomeric bacteriorhodopsin (Casadio et al., 1980), both light-adapted and dark-adapted samples are mixtures of all-*trans*, 15-*anti* and 13-*cis* (15-*syn*, assuming analogy with bacteriorhodopsin) retinal-containing chromophores (Maeda et al., 1985; Lanyi, 1986a; Oesterhelt et al., 1986; Fodor et al., 1987; Pande et al., 1989). In the dark-adapted samples the two isomeric forms are in thermal equilibrium. Sustained illumination increases the all-*trans* retinal content of the samples, and the samples return to the dark-adapted state in the absence of illumination over tens of hours at room temperature (Hazemoto et al., 1984; Lanyi, 1984; Kamo et al., 1985; Zimányi and Lanyi, 1987). Both kinds of chromophores undergo photoreactions of their own. In bacteriorhodopsin, the photocycles of all-*trans* and 13-*cis* initial states are quite different from one another (Dencher et al., 1976; Kalisky et al., 1977; Lozier et al., 1978; Harbison et al., 1984; Hofrichter et al., 1989; Gergely et al., 1994), and under most conditions only the photocycle of the all-*trans* state is associated with transport (Fahr and Bamberg, 1982). This is true also for halorhodopsin (Lanyi, 1986a). All photocycle schemes suggested for halorhodopsin have been assumed to apply to the all-*trans* initial state, which is naturally of greater interest. The possibility of contributions from the 13-*cis* photocycle to the observed spectroscopic changes have been so far neglected. We know from studies of dark-adapted bacteriorhodopsin that when the 13-*cis* chromophore is present, its photocycle is evident in the observed absorption changes (Hofrichter et al., 1989; Gergely et al., 1994). Furthermore, the observed differences of the photocycles in the presence and absence of chloride (e.g., in nitrate) imply that at less than saturating concentrations of chloride the observed transient absorbance changes will have originated from both chloride-binding and chloride-free proteins. Attributing them to a single photocycle would be erroneous. In view of these complications, we have undertaken a reexamination of the halorhodopsin photocycle, utilizing the methods of spectroscopy and data analysis developed in the last years for our studies of the bacteriorhodopsin photocycle (Lanyi, 1992, 1993).

The results we report here require a fundamental revision of the photocycle of all-*trans* halorhodopsin from *H. salinarium*, and how it is affected by chloride. If the assumption is made that the photocycles of the various forms of halorhodopsin are independent of one another, all, or at least a large part, of what was earlier termed the HR_{640} or HR_O intermediate must arise in the 13-*cis* cycle rather than in the all-*trans* cycle. Additionally, at less than saturating chloride concentrations, what was thought to be HR_O might have been at least in part the red-shifted intermediate of the photocycle of the chloride-free protein. If a red-shifted state arises at the end of the photocycle of the chloride-binding all-*trans* form of the protein, it does not accumulate in amounts detectable by our measurements. The all-*trans* photocycle in the presence of chloride is now described by the scheme, $HR\text{-}^{h\nu} \rightarrow K \Leftrightarrow L_1 \Leftrightarrow L_2 \Leftrightarrow N \rightarrow HR$, i.e., it resembles the photocycle of bacteriorhodopsin under conditions in which the Schiff base of this protein does not deprotonate, such as at pH < 3 (Mowery et al., 1979; Kobayashi et al., 1983; Váró and Lanyi, 1989), or in the D85N (Stern et al., 1989; Otto et al., 1990; Thorgeirsson et al., 1991; Kataoka et al., 1994) and D212N (Needleman et al., 1991) mutants. Although the fraction of the halorhodopsin that enters this cycle depends on the concentration of chloride, suggesting previous binding of the anion to a site that influences the photoreaction, no step in the reaction sequence was affected by chloride at concentrations between 20 mM and 2 M. The absorption band of the unphotolyzed chromophore showed distinct chloride-dependent changes, as expected if chloride bound to the protein. However, the apparent K_D for eliciting the chloride-type photocycle was considerably different from the binding constant calculated from these spectral changes.

MATERIALS AND METHODS

Halorhodopsin-containing membranes were prepared from *Halobacterium salinarium* (formerly *halobium*) strain L33, which was transformed with an independently replicating vector to be described elsewhere, that contains the *bop* promoter followed by the *hop* structural gene, including its presequence, and the novobiocin resistance gene for selection. After inoculating from a novobiocin-containing (1 μg/ml) culture (volume ratio 1/50), growth at 40°C in medium lacking novobiocin with shaking for 3–4 days was followed by centrifugation, washing of the cells in 25% NaCl, and dialysis against 40 volumes of water in the presence of DNAse I. The lysed cells were centrifuged at 30,000 rpm for 1 h, washed with 0.1 or 0.2 M NaCl, and the resulting membrane fragments were collected in a discontinuous sucrose gradient containing 0.1 or 0.2 M NaCl, as described for purple membranes (Oesterhelt and Stoeckenius, 1974). Because unphysiologically low salt concentration was used to disrupt the halophilic cells, the preparation contained membrane fragments rather than closed vesicles. The absorbance ratio at 280 and 580 nm was approximately 4, indicating that approximately one-half of the protein in these membranes was halorhodopsin. A small

extent of contamination with cytochrome that has an absorption band at approximately 415 nm (see legends to Figs. 4–7) was tolerated. The membrane fragments collected from the gradients were stored without removing the sucrose at −70°C and centrifuged, washed, and resuspended in the buffer of choice before use, similarly to purple membranes. Solubilized halorhodopsin was prepared as described earlier (Duschl et al., 1988).

Flash excitation with a frequency-doubled Ne-Yag laser and measurement of absorption changes with an intensified diode array and at single wavelengths were as previously described (Zimányi et al., 1989a; Váró and Lanyi, 1991a; Zimányi and Lanyi, 1993), except that in the latter measurements a photomultiplier with extended sensitivity in the red was used. Some of the noise in the time-resolved difference spectra was removed by singular value decomposition (SVD) (Golub and Kahan, 1995). In some cases, the rate constants of the photocycle reactions were obtained by comparing the measured single-wavelength absorbance changes with simulations of a program that generates single-wavelength kinetics for any photocycle model, given the extinction coefficients of the intermediates. The dark- or light-adapted states of the samples during the spectroscopic measurements were ensured by the use of a step-pump that replaced the contents of the cuvette after each flash with a fresh sample from a reservoir (Gergely et al., 1994) containing either previously dark-adapted or continuously illuminated (with white light) halorhodopsin-containing membranes. All experiments were performed in the presence of 50 mM 2-(2-morpholino)ethane sulfonic acid (MES), pH 6.0, in addition to the other salts present as specified. The total cation concentration of the salts added was 2 M. The temperature was regulated at 22°C throughout.

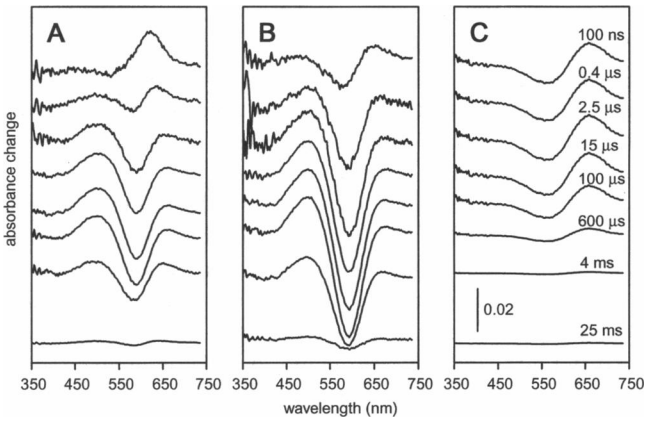

FIGURE 1 Measured difference spectra for halorhodopsin-containing membrane fragments under three conditions. The spectra were measured at the indicated delay times after photoexcitation, with optical multichannel spectroscopy. (*A*) and (*B*) 2 M NaCl. (*C*) 1 M Na_2SO_4. (*A*) Dark-adapted sample. (*B*) and (*C*) Light-adapted samples. In sulfate the spectra of dark-adapted and light-adapted samples were superimposable. The halorhodopsin concentration was 15 µM in each case.

RESULTS

Resolving the flash-induced spectral changes of the different initial states of halorhodopsin

In a heterogeneous system, such as halorhodopsin, extracting the many time constants and amplitudes by global fitting of spectral data is not a promising strategy for separating the multiple photocycles that contribute to the absorption changes. Instead, we created conditions in which one or another of the photocycles dominated and attempted to calculate the spectra and kinetics associated with each of the postulated initial states.

One of the principal questions was what conditions should be used for the reference chloride-free state for the comparisons with the chloride-binding state. The halorhodopsin-containing membrane fragments used in this study were nearly equivalent to the purple membranes that contain only bacteriorhodopsin and lipids, although, unlike the latter, they showed no two-dimensional crystalline structure. Although not immobilized by a lattice, the halorhodopsin chromophore in these membranes was much more stable than the earlier purified preparations in detergent micelles, particularly when illuminated in the absence of chloride or nitrate. The latter condition could be obtained therefore in the presence of sulfate, an anion that does not interact significantly with halorhodopsin (Schobert et al., 1986; Schobert and Lanyi, 1986), at concentrations sufficient to maintain a constant amount of cation up to several molar. With these preparations we could thus compare the spectral changes that occur upon photoexcitation in NaCl and in Na_2SO_4 (at a constant 2 M $[Na^+]$) and in the initially dark-adapted and light-adapted states. Fig. 1 shows difference spectra at a few selected delay times after flash excitation for dark-adapted halorhodopsin in 2 M NaCl (panel *A*), light-adapted halorhodopsin in 2 M NaCl (panel *B*), and for halorhodopsin in 1 M Na_2SO_4 in which light adaptation had no detectable effect on the spectra (panel *C*). Fig. 1, *A* and *B*, demonstrates that, as in bacteriorhodopsin, the photocycles of the two components present, containing all-*trans* and 13-*cis* retinal, are greatly different. The main difference is that, in the light-adapted samples, when the ratio of these is shifted toward all-*trans* (Hazemoto et al., 1984; Lanyi, 1984; Kamo et al., 1985; Zimányi and Lanyi, 1987), the amplitude of the red-shifted state(s) in the spectra is decreased and that of the blue-shifted state(s) is increased.

In bacteriorhodopsin, the light-adapted state contains 100% all-*trans* retinal, which had simplified the description of its photocycle. In halorhodopsin, the light-adapted state contains significant amounts of 13-*cis* retinal (Hazemoto et al., 1984; Lanyi, 1984; Kamo et al., 1985; Zimányi and Lanyi, 1987). Resolution of the measured difference spectra in Fig. 1, *A* and *B*, into the contributions of the all-*trans* and 13-*cis* forms would require knowing not only the ratio of the retinal isomers in the dark- and light-adapted states, but also the relative extinctions of the two forms at the wavelength of the flash and the relative quantum yields for the two photocycles. The all-*trans* retinal content, determined in these samples by retinal extraction, is 48% when dark adapted and 79% when light adapted (Váró, Sasaki, Maeda, Needleman, and Lanyi, manuscript in preparation). We used a different approach instead. We noted that, by fortunate coincidence, at wavelengths above ~680 nm, the amplitudes of the difference spectra after ~100 µs were virtually the same in dark-adapted and light-adapted samples (see inset to Fig. 2). This means that, because the large differences in the spectra at lower wavelengths indicate large differences in the all-*trans*/13-*cis* ratio, at >680 nm, the individual amplitudes of the difference spectra for the two forms must be essentially the same. In the case of the 13-*cis* cycle, this is apparently a result mostly of red-shift of the spectra of the intermediates

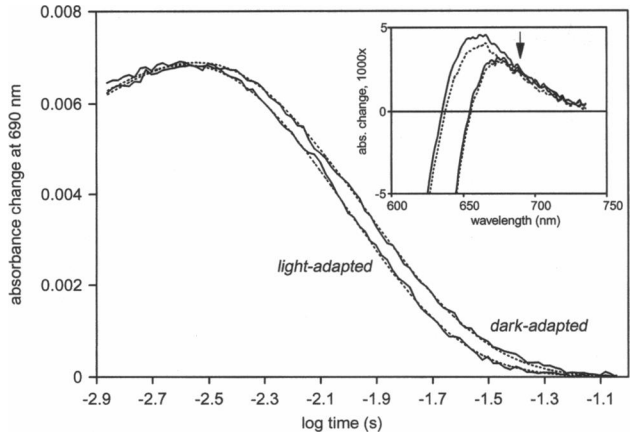

FIGURE 2 Time dependence of absorbance change at 690 nm after photoexcitation of light-adapted and dark-adapted samples in 2 M NaCl. Inset, difference spectra (as in Fig. 1, *A* and *B*) at 1.5 ms (solid lines) and 4 ms (broken lines). The two spectra with larger amplitudes are from light-adapted and those with smaller amplitudes are from dark-adapted samples. The arrow indicates the position of 690 nm.

and, in the all-*trans* cycle, to broadening of the spectra (see below). The kinetics of the absorption change at a suitable wavelength in this region, e.g., 690 nm, could be fitted with the same two exponential components in the light-adapted and the dark-adapted states (the measured traces in the body of Fig. 2 are the solid lines, and the fits are the dashed lines). Their time constants were 8 and 14 ms, whereas the fractional amplitudes were 0.47 ± 0.04 and 0.53 ± 0.04 in the dark-adapted state and 0.84 ± 0.07 and 0.16 ± 0.02 in the light-adapted state. The 8- and 14-ms components thus appear to correspond to the decay process in the all-*trans* and the 13-*cis* cycles, respectively. Because the individual amplitudes of the changes in the all-*trans* and 13-*cis* cycles are the same, the resolved amplitudes of the two kinetic components give directly the fractions of halorhodopsin that pass through the two photocycles. It turns out that they correspond reasonably closely to the isomeric ratios (Váró, Sasaki, Maeda, Needleman, and Lanyi, manuscript in preparation).

According to this analysis, the contribution of the all-*trans* cycle to the difference spectra in Fig. 1, *A* and *B*, is 0.47 when dark adapted and 0.84 when light adapted. The all-*trans* retinal contents of dark-adapted and light-adapted halorhodopsin in the somewhat comparable cell envelope vesicles were reported to be 24 and 61%, respectively (Lanyi, 1986a). If the photocycles are independent of one another (the consequences of the alternative, that the photocycles share intermediate(s), will be examined in a separate study), each pair of measured difference spectra, *sp*(DA) and *sp*(LA) in Figs. 1A and B, is described by the equations:

$$sp(\mathrm{DA}) = a \times sp(\text{all-}trans) + (1 - a) \times sp(13\text{-}cis) \quad (1)$$

$$sp(\mathrm{LA}) = b \times sp(\text{all-}trans) + (1 - b) \times sp(13\text{-}cis), \quad (2)$$

where *a* and *b* are the fractional contributions of all-*trans* form in the dark-adapted and light-adapted states, respectively. Solving for *sp*(all-*trans*) and *sp*(13-*cis*) produced the difference spectra in Fig. 3, *A* and *B*. They constitute the spectral changes of the all-*trans* and 13-*cis* forms in the presence of chloride.

Such a resolution of the all-*trans* and 13-*cis* photocycles is the key to solving the photoreaction of halorhodopsin, and we took pains to make certain that it was valid. Because the relaxation times of 8 and 14 ms in the two cycles are not greatly different from one another, making the biexponential fit (Fig. 2) and the calculation of *a* and *b* difficult, it was reassuring that the calculated spectra were fairly tolerant to inaccuracies in the time constants. For example, changing and fixing the relaxation times at the best fits ±15% changed the calculated values of *a* and *b* by only ~2% and altered the calculated spectra to negligible extents. A general criterion of successfully separating two independent reaction sequences is that the number of time constants in the two resolved sequences be minimized. SVD analysis (see below) showed that forcing *a* and *b* to be significantly different from the values given above resulted in nonnegligible amplitudes for the 8-ms time constant in what was calculated to be the 13-*cis* photocycle and the 14-ms time constant in the resulting all-*trans* cycle.

The measured spectra in Fig. 1 *C*, which do not change upon light adaptation, refer to the changes in the absence of chloride. It is not clear why only one photocycle is seen under the latter condition, as both isomeric forms of the retinal are present also in the absence of chloride (Lanyi, 1986a). We anticipate that time-resolved infrared spectroscopy of these photoproducts will address the possibility that the quantum yield of one of the two isomeric forms might be much smaller than the other.

The spectral analysis of the photocycle in 2 M NaCl was carried out with purified dark-adapted and light-adapted halorhodopsin in octylglucoside-cholate micelles (Duschl et

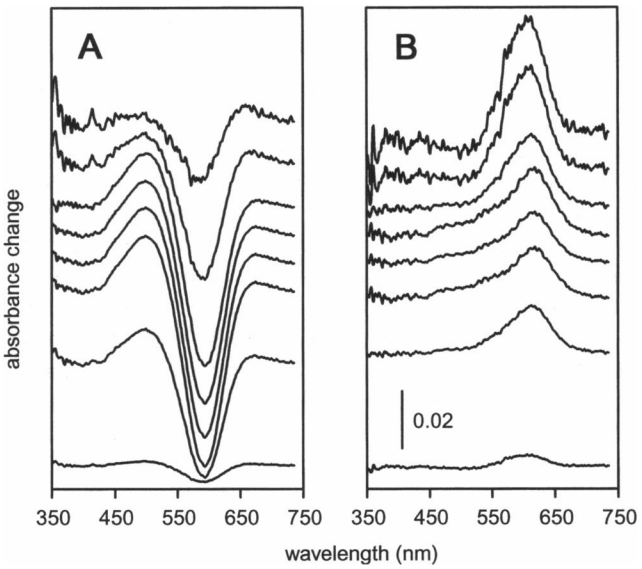

FIGURE 3 Calculated difference spectra for the resolved all-*trans* (*A*) and 13-*cis* (*B*) photocycles in 2 M NaCl. The delay times are the same as in Fig. 1.

al., 1988) as well (not shown). Estimation of the relative contributions of the all-*trans* and 13-*cis* photocycles to the difference spectra was hindered by the fact that the time constants of the final decay at 690 nm (as in Fig. 2) were not sufficiently different in the two cycles to treat the decay as a biexponential process. However, difference spectra for the pure all-*trans* and 13-*cis* cycles very similar to those in Fig. 3 were obtained from calculations based on 47% contribution of the all-*trans* cycle to the dark-adapted spectra (i.e., as in the membrane fragments) and 60% contribution to the light-adapted spectra (i.e., somewhat less than in the membrane fragments). A 60% all-*trans* content in the light-adapted state is similar to what was determined earlier by retinal extraction of detergent-solubilized halorhodopsin (Maeda et al., 1985) and halorhodopsin-containing proteoliposomes (Zimányi and Lanyi, 1987). It is consistent also with the observation that detergent solubilization decreases the amount of all-*trans* retinal in light-adapted bacteriorhodopsin (Casadio et al., 1980).

Kinetic models for the three halorhodopsin photocycles

We note that, according to Fig. 3 in chloride-containing samples, most, although not all, of the absorption increase in the red region originates from the 13-*cis* component, whereas all of the increase in the blue originates from the all-*trans*. The spectra assigned to the photocycle of the 13-*cis* form resemble those in the photocycle of 13-*cis* bacteriorhodopsin and show only absorbance increase (Gergely et al., 1994). The changes in the absence of chloride also consist of increases in the red region (Fig. 1 *C*), but these appear to have originated from a red-shift of the maximum rather than solely from an amplitude increase.

The number of independent spectral components in each of the three sets of data (31 spectra/set) were first estimated from SVD (Golub and Kahan, 1995). In the set for the all-*trans* photocycle, only the first two basis spectra (u columns) and their time dependencies (v columns) were significantly above noise. This is indicated also by the fact that the pairwise products of the correlations of the first three u and v columns were 0.93, 0.60, and −0.05, respectively. Although a rank of two would suggest that two intermediates are present, there were three well separated time constants in the kinetics, indicating that there should be one more. Indeed, with two spectra, the decay of the first putative intermediate was followed by its rise, giving an unlikely kinetic scheme. In the data set for the 13-*cis* photocycle, the SVD analysis suggested also two intermediates, the products of the correlations of the first three being 0.95, 0.51, and −0.1. The kinetics in this case contained only two time constants. In the set for the photocycle in sulfate, the products of the correlations were 0.93 and 0.39 and suggested that if there is a second intermediate it cannot be clearly distinguished with available signal/noise.

Given these constraints, we calculated the spectra of the three presumed intermediates of the all-*trans* cycle of the chloride-binding form of halorhodopsin from time-resolved difference spectra, such as in Fig. 3 *A*. The search for these spectra was based on the criteria of not allowing negative absorption, and limits on the amplitude and half-width of the resulting spectra, much as before for bacteriorhodopsin (Váró and Lanyi, 1991a; Zimányi and Lanyi, 1993). The estimated spectra, shown in Fig. 4 *A*, are labeled K, L, and N in analogy with the intermediates of the photocycle of bacteriorhodopsin under conditions in which no M intermediate accumulates. When, for the sake of simplicity, we refer to a K state, it is the one earlier described as KL (Zimányi et al., 1989a,b; Zimányi and Lanyi, 1989a) in analogy with a proposed late K substate in the bacteriorhodopsin photocycle (Shichida et al., 1983). Although it can be argued that using the designations for the bacteriorhodopsin photointermediates for halorhodopsin is misleading because their equivalency has not yet been demonstrated, the alternative terminology that utilizes the absorption maxima is also confusing because the calculated spectra and absorption maxima of the intermediates varies considerably among different

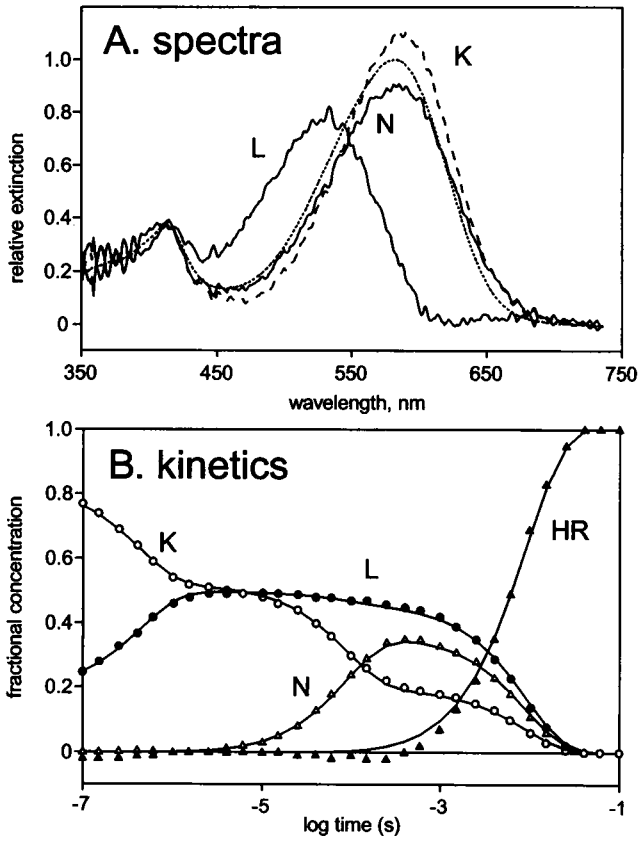

FIGURE 4 Calculated spectra of all-*trans* halorhodopsin and its photointermediates (*A*) and the kinetics of its photocycle (*B*) in 2 M NaCl. The spectrum of unphotolyzed halorhodopsin is shown in *A* with broken line, that of the K intermediate with dashed line. The small band at 415 nm is from the cytochrome content of the membrane fragments. Symbols in *B*: ○, K intermediate; ●, L intermediate; △, N intermediate; ▲, HR (i.e., 1 minus the sum of the concentrations of all intermediates). The solid lines in *B* represent the best fit of the model $K \Leftrightarrow L_1 \Leftrightarrow L_2 \Leftrightarrow N \rightarrow HR$, with the rate constants listed in Table 1.

publications. The spectra for K and N differ primarily in amplitude, consistent with the fact that SVD analysis distinguished only two spectral components (see above). The spectrum of N is broader than the others, and its red-edge accounts for the persistence of a small absorption increase above 650 nm in the millisecond time range despite the decay of the K intermediate (Fig. 3 *A*).

The measured difference spectra were decomposed into mixtures of the K minus HR, L minus HR, and N minus HR spectra. The fractional concentrations of these components are shown as functions of delay time in Fig. 4 *B* (symbols). The points labeled as HR (1 minus the sum of all components) are reasonably close to the zero line until the beginning of the recovery of the initial state at ~1 ms, indicating that the calculated spectra do describe the components that make up all of the data despite the fact that their proportions change with time. This is a stringent criterion for the validity of the calculated spectra (Zimányi and Lanyi, 1993). However, we recognize that small uncertainties in the spectra may produce uncertainties in the kinetics.

The simplest kinetic scheme would be $K \Leftrightarrow L \Leftrightarrow N \rightarrow HR$. However, this scheme introduced a contradiction. As shown in Fig. 4 *B*, the initial equilibration of K with L at a few microseconds resulted in a 1:1 mixture of K and L, but in the equilibration of K, L, and N that followed it at a few hundred microseconds, the [K]/[L] ratio decreased to approximately 1/2. The χ^2 of the fit of this scheme (not shown) was 0.14. The same kind of paradox, but for the L and M intermediates, turned up in the bacteriorhodopsin photocycle (Váró and Lanyi, 1991a,b; Zimányi et al., 1992; Zimányi and Lanyi, 1993), and its solution was the introduction of two M substates connected by a unidirectional reaction. Two sequential L substates will solve the problem in halorhodopsin also, but in this system the K intermediate persists until the recovery of the initial state, and thus the reaction between the putative L substates will not be unidirectional. The lines in Fig. 4 *B* represent the best fit of the scheme $K \Leftrightarrow L_1 \Leftrightarrow L_2 \Leftrightarrow N \rightarrow HR$ with the rate constants given in Table 1 (column for 2.0 M NaCl). The χ^2 of this fit was substantially improved at 0.012. The rate constants of the $L_2 \Leftrightarrow N$ equilibration are not defined by the data, beyond the requirement that the forward constant be greater than $2 \times 10^7\ s^{-1}$ and the reverse be greater than $1.3 \times 10^7\ s^{-1}$ and that $[N]/[L_2]$ at equilibrium be 1.50.

The model with sequential L substates is not the only option. Three other models based on $K \Leftrightarrow L_1 \Leftrightarrow N \rightarrow HR$, with a cul-de-sac leading to equilibration of L_2 with either K, L_1, or N gave equivalent χ^2 values, between 0.011 and 0.013. Similarly, the sequence $K \Leftrightarrow L_1 \Leftrightarrow L_2 \rightarrow HR$ plus $L_2 \Leftrightarrow N$ gave an equally satisfactory fit. Identification of the correct model among these (and others that are more complex) will have to be on the basis of additional information, such as the altered photocycles of site-specific mutants in the case of bacteriorhodopsin. In the meantime, we suggest that the $K \Leftrightarrow L_1 \Leftrightarrow L_2 \Leftrightarrow N \rightarrow HR$ sequence will serve as a reasonable working model for the all-*trans* photocycle.

Analogous treatment of the spectra for the 13-*cis* cycle, such as in Fig. 3 *B*, produced the spectra and kinetics in Fig. 5, *A* and *B* (symbols). The detected intermediates termed CIS-1 and CIS-2 have spectra similar to those of the 13-*cis* bacteriorhodopsin photocycle (Gergely et al., 1994). The kinetics are simple and can be described with the scheme CIS-1 $\Leftrightarrow$ CIS-2 $\rightarrow$ HR (lines in Fig. 5 *B*). This kinetic scheme is mathematically equivalent to two parallel photoreactions or one photoreaction with two branches, one containing CIS-1 and the other CIS-2, and we cannot distinguish between the first model and these. A branched scheme was suggested to reflect the crossover of the 13-*cis* photocycle of bacteriorhodopsin to the all-*trans*, i.e., the phenomenon of light adaptation (Gergely et al., 1994).

Fig. 6, *A* and *B* (symbols), show the calculated spectra and kinetics for the halorhodopsin photocycle in Na_2SO_4. Within error, only one spectrally distinct intermediate results, which is shifted considerably further to the red than either intermediate in the 13-*cis* cycle of the chloride-binding form. It arises faster than 100 ns and decays with either a single exponential (solid line in Fig. 6 *B*) or two exponentials of not very different time constants (dashed line). The latter treatment would suggest two parallel processes.

Chloride-dependent spectral changes in unphotolyzed halorhodopsin

The difference of the photochemical cycles measured in chloride and sulfate (Fig. 1) indicates that chloride affects the photoreaction. The simplest way this could happen would be the binding of chloride to the unphotolyzed

TABLE 1 Rate constants of best fit for the photocycle of all-trans halorhodopsin at various chloride concentrations

Reaction	Chloride concentration (M)						
	0.020	0.050	0.100	0.200	0.500	1.000	2.000
$K \rightarrow L_1$	1.3×10^6	1.3×10^6	1.3×10^6	1.3×10^6	1.3×10^6	1.3×10^6	1.3×10^6
$L_1 \rightarrow K$	1.0×10^6	1.0×10^6	1.1×10^6	1.3×10^6	1.3×10^6	1.3×10^6	1.3×10^6
$L_1 \rightarrow L_2$	1.4×10^4	1.4×10^4	1.4×10^4	1.4×10^4	1.4×10^4	1.4×10^4	1.4×10^4
$L_2 \rightarrow L_1$	0.9×10^4	0.9×10^4	0.9×10^4	0.9×10^4	0.9×10^4	0.9×10^4	0.9×10^4
$L_2 \rightarrow N$	$\geq 2 \times 10^7$	$\geq 2 \times 10^7$	$\geq 2 \times 10^7$	$\geq 2 \times 10^7$	$\geq 2 \times 10^7$	$\geq 2 \times 10^7$	$\geq 2 \times 10^7$
$N \rightarrow L_2$	$\geq 1.3 \times 10^7$	$\geq 1.3 \times 10^7$	$\geq 1.3 \times 10^7$	$\geq 1.3 \times 10^7$	$\geq 1.3 \times 10^7$	$\geq 1.3 \times 10^7$	$\geq 1.3 \times 10^7$
$N \rightarrow HR$	5.0×10^2	3.3×10^2	3.3×10^2	2.8×10^2	2.8×10^2	2.8×10^2	2.8×10^2

Rate constants are in s^{-1}.

The fits required that the ratio of $k_{L2 \rightarrow N}$ to $k_{N \rightarrow L2}$ be 1.5.

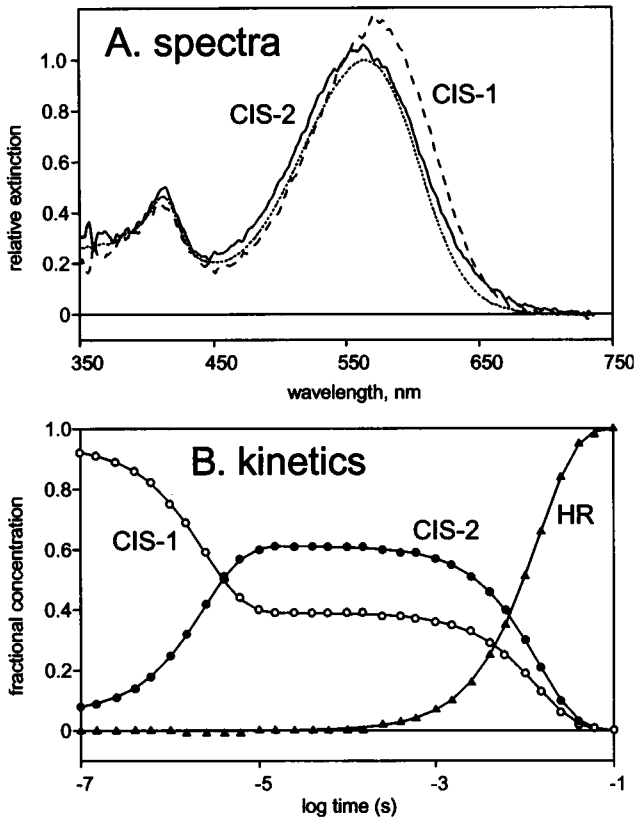

FIGURE 5 Calculated spectra of 13-*cis* halorhodopsin and its photointermediates (*A*) and the kinetics of its photocycle (*B*) in 2 M NaCl. The spectrum of unphotolyzed halorhodopsin is shown in *A* with broken line, that of the CIS-1 intermediate with dashed line. The small band at 415 nm is from the cytochrome content of the membrane fragments. Symbols in *B*: ○, CIS-1 intermediate; ●, CIS-2 intermediate; △, HR (i.e., 1 minus the sum of the concentrations of the two intermediates). The solid lines in *B* represent the best fit of the model CIS-1 ⇔ CIS-2 → HR, with the rate constants (in s^{-1}), $k_{CIS\text{-}1 \rightarrow CIS\text{-}2} = 2.6 \times 10^5$, $k_{CIS\text{-}2 \rightarrow CIS\text{-}1} = 1.6 \times 10^5$, and $k_{CIS\text{-}2 \rightarrow HR} = 1.2 \times 10^2$.

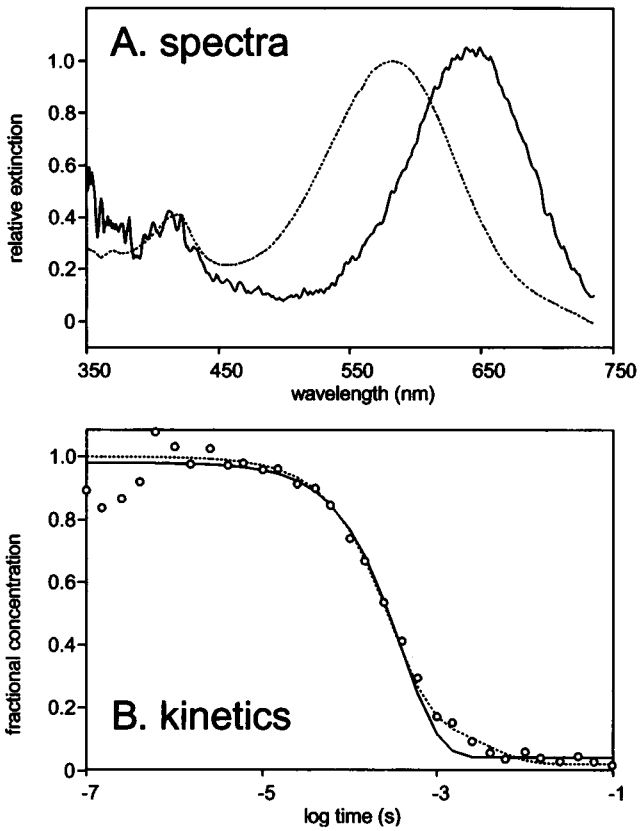

FIGURE 6 Calculated spectra of halorhodopsin and its photointermediates (*A*) and the kinetics of its photocycle (*B*) in 1 M Na_2SO_4. The spectrum of unphotolyzed halorhodopsin is shown in *A* with broken line. The small band at 415 nm is from the cytochrome content of the membrane fragments. ○, the single intermediate detected. Solid line, exponential decay with τ = 396 μs; broken line, biexponential decay with τ_1 = 308 μs and τ_2 = 3.8 ms.

protein. Such binding had been postulated on the basis of spectral shifts in chloride versus nitrate in visible spectra (Ogurusu et al., 1982, 1984; Lanyi and Schobert, 1983; Schobert et al., 1983; Steiner et al., 1984) and in vibrational spectra (Maeda et al., 1985; Rothschild et al., 1988; Pande et al., 1989) and broadening of the ^{35}Cl NMR line (Falke et al., 1984). Because the chromophore was fairly stable in the membrane fragments used here even in the absence of chloride, we could determine spectral changes in chloride versus sulfate with accuracy. Fig. 7 *A* shows that removing chloride caused a considerable decrease in the amplitude of the absorption band, an increase in its width, and a moderate blue-shift of its maximum (from 580 to 570 nm). These changes were reversible upon adding chloride. The amplitude change, plotted as a fraction of the amplitude increase at 2 M NaCl (i.e., at presumed saturation) as a function of chloride concentration gives an apparent K_D of 20 mM (Fig. 7 *B*, open circles). The shift of the maximum appears to be a separate effect, but its concentration dependence could not be determined.

The chloride dependence of the amplitude of the photocycles associated with chloride, described above, was also determined. Three wavelengths were selected that best distinguish the absorbance changes of the chloride-binding protein from those of the chloride-free form. The absorbance changes of the photocycle in sulfate exhibit a zero crossover point at 611 nm (see below), and any changes at this wavelength at various chloride concentrations will have necessarily originated from the chloride-binding form only, thus describing its dependence on [Cl^-]. At 590 and 660 nm, part of the absorbance changes originate from the chloride-free form, but when the amplitudes are rescaled to zero in 1 M sulfate and one in 2 M NaCl, the fractional values at intermediate chloride concentrations also describe the dependence on [Cl]. Fig. 7 *B* contains plots of these three measured parameters versus [Cl]. The apparent K_D for the photocycle amplitude is 80 mM, i.e., significantly higher than the K_D for the chloride-dependent spectral change of the unphotolyzed chromophore. A similar conclusion was made from spectral measurements with lipid-reconstituted halorhodopsin (Zimányi and Lanyi, unpublished experiments).

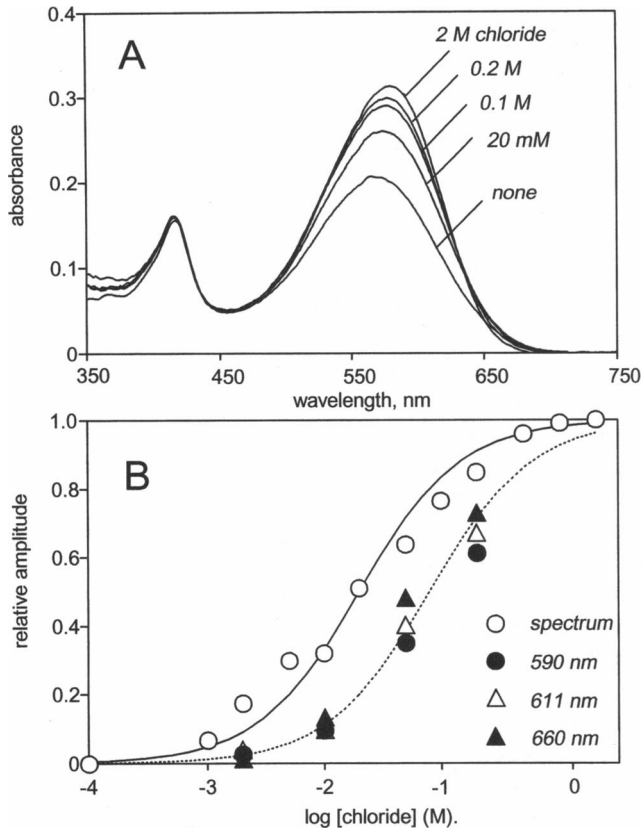

FIGURE 7 Chloride dependence of the spectral shape of unphotolyzed halorhodopsin (*A*) and amplitudes of absorbance changes after photoexcitation at three different wavelengths (*B*). In *A*, spectra of matched samples (light-adapted halorhodopsin-containing membranes) are shown in mixtures of NaCl and Na_2SO_4 (total Na^+ concentration, 2 M). The small band at 415 nm is from the cytochrome content of the membrane fragments. In *B*, various chloride-dependent parameters are plotted versus the chloride concentration. The chloride-dependent changes were normalized to a scale between zero in sulfate and one in 2 M chloride. ○, amplitude change in A; ●, maximal amplitude change after photoexcitation when measured at 590 nm; △, maximal amplitude change after photoexcitation when measured at 611 nm; ▲, maximal amplitude change after photoexcitation when measured at 660 nm.

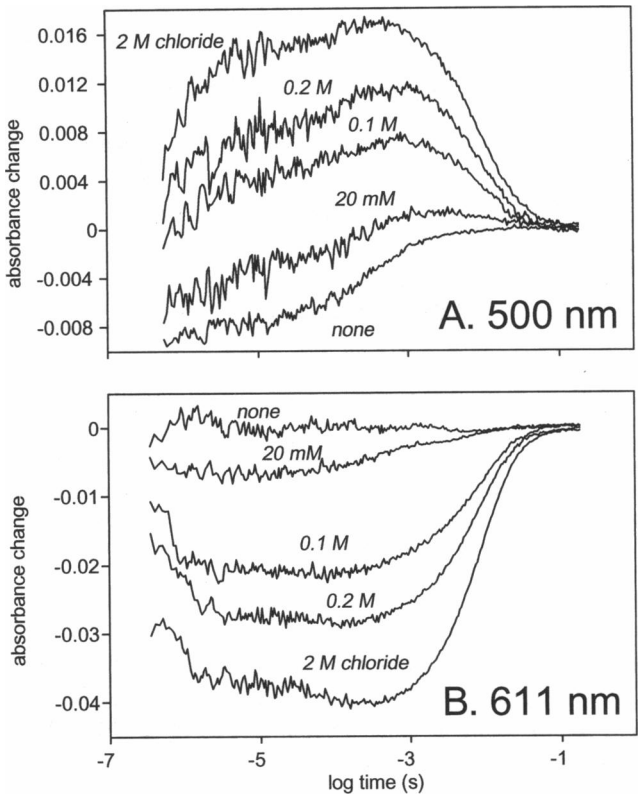

FIGURE 8 Traces of absorbance change at 500 nm (*A*) and 611 nm (*B*) after photoexcitation of light-adapted halorhodopsin (15 μM) in 2 M NaCl.

The all-*trans* photocycle of the chloride-bound form of halorhodopsin at different chloride concentrations

It had been shown before that, as in bacteriorhodopsin, it is the photocycle of the all-*trans* isomeric form of halorhodopsin, containing the distinct blue-shifted intermediate described here as L, that results in transport of chloride (Lanyi et al., 1990b). Inasmuch as this photocycle originates from the chloride-binding form of the protein, its overall amplitude indeed increases with chloride concentration (Fig. 7 *B*). If there is additionally a chloride-dependent rate constant in this cycle, its presence will reveal the release or uptake of chloride after the photoexcitation. We have examined therefore the rate constants in the model for the all-*trans* photocycle at chloride concentrations between 20 mM and 2 M.

For this study we used single wavelength spectroscopy and, at each chloride concentration, measured the absorbance changes of a dark-adapted and a light-adapted sample. It was assumed that the photocycles of the chloride-binding and chloride-free forms are independent. Fig. 8, *A* and *B*, show traces of the time dependence of absorbance change at 500 and 611 nm, respectively, for a light-adapted sample at various chloride concentrations. At 611 nm, there is no contribution from the photocycle of the chloride-free form and, within error, only the amplitude of the traces is dependent on chloride. Thus, none of the time constants of the photocycle evident at 611 nm are dependent on chloride (compare below). At this wavelength, however, both all-*trans* and 13-*cis* photocycles contribute. As in both light-adapted and dark-adapted samples it was only the amplitude of the traces that was dependent on chloride, the fractional contribution of the all-*trans* cycle must be independent of the chloride concentration. At 500 nm, the photocycle of the chloride-free protein contributes a negative signal, whereas the cycles of the chloride-binding forms make a positive contribution. The amplitudes of the traces at 611 nm could be used, therefore, to extract from the data at 500 nm the contribution of the chloride-binding protein. Comparing traces for light-adapted and dark-adapted samples, in turn, allowed the calculation of the changes due only to the all-*trans* photocycle, as in the case of the time-resolved spectra above. Fig. 9 shows traces for the all-*trans* cycle in 1 M NaCl calculated in this way at 500, 630, and 611 nm. Global fitting of the kinetic scheme $K \Leftrightarrow L_1 \Leftrightarrow L_2 \Leftrightarrow N \rightarrow HR$ to such triple traces at various chloride concentrations yielded the set of rate constants given

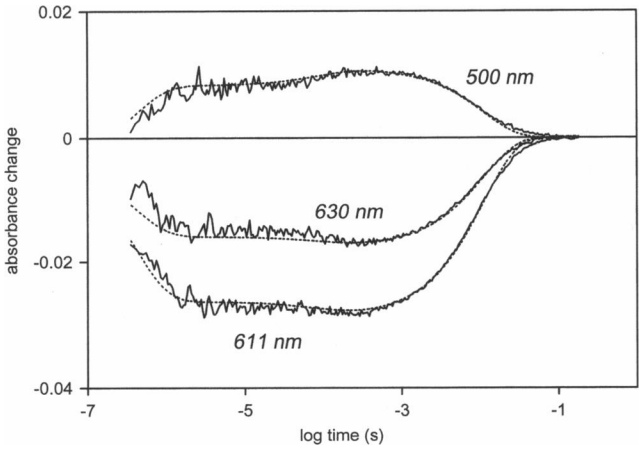

FIGURE 9 Calculated absorbance changes in the photocycle of the all-*trans* chloride-binding protein at 500, 630, and 611 nm in 1 M NaCl plus 0.5 M Na_2SO_4. The solid lines represent the best fit of the model $K \Leftrightarrow L_1 \Leftrightarrow L_2 \Leftrightarrow N \rightarrow HR$, with the rate constants listed in Table 1.

in Table 1. The five fully determined rate constants are chloride independent within error. As far as we can tell, the two less determined rate constants in the $L_2 \Leftrightarrow N$ equilibrium are also unaffected by chloride.

DISCUSSION

We have resolved the multiple photocycles that originate from the isomeric and chloride-binding heterogeneity of halorhodopsin, with the only assumption that the observed transient absorption changes originate from independent photochemical reactions. The objective was to describe the photochemical cycle associated with the transport of chloride. Given the facts that the light-adapted chromophore contains significant amounts of 13-*cis* retinal, and the time-resolved absorption changes are greatly affected by light adaptation, there can be no doubt that a contribution of the 13-*cis* photocycle is present in the measured absorption changes and must be removed when describing the photoreaction of the all-*trans* chromophore. For this reason the photocycle of the 13-*cis* chromophore was also described. In the absence of chloride, only one photocycle was detected. It is different from the two cycles of the chloride-binding form. We needed to describe it to extract the photocycle of the chloride-binding form at subsaturating concentrations of chloride. With this approach the transient absorption changes of light- and dark-adapted samples at different chloride concentrations could be represented as various linear combinations of three photocycles with unchanging kinetic parameters, within measurement error, consistent with the assumed absence of cross-reactions.

The results demonstrate that the photochemical changes of the all-*trans* chromophore in the chloride-binding protein greatly resemble those of bacteriorhodopsin under conditions in which the Schiff base is prevented from deprotonating. This seems reasonable in view of the similarity of halorhodopsin and bacteriorhodopsin and the lack of a proton acceptor to the Schiff base in the former protein. The photocycle is described by the scheme $HR\text{-}^{h\nu} \rightarrow K \Leftrightarrow L_1 \Leftrightarrow L_2 \Leftrightarrow N \rightarrow HR$. The two L substates may play the same role in the chloride transport as the two M substates in the proton transport in bacteriorhodopsin (Váró and Lanyi, 1991b; Kataoka et al., 1994). If they do, the internal translocation of chloride occurs during the lifetime of the L states. None of the intermediates that accumulate absorb as far to the red of the main band of halorhodopsin as the previously identified HR_{640} or O state. Although the existence of such an intermediate cannot be rigorously excluded, it seems now that all or most of it originates in the 13-*cis* photocycle and the photocycle of the chloride-free form. Placing the detected red-shifted intermediate in the all-*trans* photocycle was due to artifact. It was based on the observation of absorption rise in the red region and concurrent absorption decrease in the blue region, in the several-millisecond time domain. The postulated slow chloride-dependent equilibration of a blue-shifted and red-shifted intermediate seemed to identify chloride release of likely relevance in the transport. However, we find that these changes originate from the fact that the L to N conversion in the all-*trans* cycle removes depletion, masking the more slowly decaying red-shifted intermediate of the 13-*cis* cycle. Indeed, particularly when viewed on a logarithmic time scale, the amplitude of this rise in the red region relative to the increased absorbance level (from the 13-*cis* cycle) becomes smaller and smaller when the measuring light is set to longer and longer wavelengths. This is partly evident from the smallness of the amplitude of the rising phase at 690 nm in Fig. 2. Above 700 nm, little or no absorption rise in the millisecond time domain, over the level established at much shorter times, was seen (not shown). On repeating these experiments with solubilized halorhodopsin, we found a similar wavelength dependence of the millisecond kinetics (not shown).

The absorption changes upon chloride binding to the unphotolyzed protein are more complex than previously thought. When the chloride-free reference state of the protein is sulfate, chloride causes an increase of the extinction of the main band, narrowing of the band-width, and an approximately 10-nm red-shift of the maximum (Fig. 7 *A*). This is similar to the effect of chloride on the width of the absorption band of D212N bacteriorhodopsin (Brown and Lanyi, unpublished experiments), i.e., in a mutant in which chloride binding might be also the consequence of the net positive charge of the extracellular protein domain. However, the red-shift of the maximum is inconsistent with binding of the chloride near the Schiff base, as pointed out before from the direction of the chloride-dependent shift of the resonance Raman C = N stretching band (Pande et al., 1989). The apparent K_D for the absorption amplitude change is significantly different than that for the amplitude of the photocycle associated with the chloride-binding forms of the protein (Fig. 7 *B*). A possible explanation would be that the chloride that affects the photocycle amplitude is bound subsequent to rather than before the photoexcitation. However, this binding would have had to occur well before 100 ns because the first

intermediate detected in the absence of chloride is considerably different from that detected in the presence of chloride (compare Figs. 4 *A*, 5 *A*, and 6 *A*). This seems unlikely. The alternative explanation is that there are more than one chloride binding site, with different effects on the spectrum of the unphotolyzed chromophore and its photoreaction. The apparent binding constant we now find for the chloride effect on the photoreaction is similar to the K_D for freely exchanging chloride determined from ^{35}Cl NMR line broadening (Falke et al., 1984), for which previously no equivalent was found with spectroscopy in the visible. Interestingly, adding chloride to halorhodopsin from *Natronobacterium pharaonis* causes blue-shift rather than red-shift of the absorption maximum, although qualitatively the same chloride-dependent changes are found in the photocycle (Scharf and Engelhard, 1994) as in *H. salinarium*.

To our disappointment, the all-*trans* photocycle, which must be associated with chloride transport, does not contain any chloride-dependent rate constants that might serve as clues to where chloride is taken up or released (Table 1). We regard the relationship of this photochemical cycle to the mechanism of chloride transport therefore as a still entirely open question. It will be understood only by identifying the partial chloride transfer reactions with site-specific mutations studied with vibrational spectroscopy in addition to spectroscopy in the visible, analogously to the way the mechanism of proton transport is being uncovered in bacteriorhodopsin.

This work was funded by grants from the National Institutes of Health (GM 29498 to J.K.L.), the National Science Foundation and the U.S. Army Research Office (MCB-9202209 and DAAL03–92-G-0406 to R.N.), and the National Scientific Research Fund of Hungary (OTKA T5073 to G.V., L.Z., and J.K.L.).

REFERENCES

Ames, J. B., J. Raap, J. Lugtenburg, and R. A. Mathies. 1992. Resonance Raman study of halorhodopsin photocycle kinetics, chromophore structure, and chloride-pumping mechanism. *Biochemistry.* 31:12546–12554.

Blanck, A., and D. Oesterhelt. 1987. The halorhodopsin gene. II. Sequence, primary structure of halorhodopsin, and comparison with bacteriorhodopsin. *EMBO. J.* 6:265–273.

Bogomolni, R. A. 1984. Photochemical reactions of halorhodopsin and slow rhodopsin. *In* Information and Energy Transduction in Biological Membranes. A. Bolis, H. Helmreich, and H. Passow, editors. Alan R. Liss, New York. 5–12.

Braiman, M. S., T. J. Walter, and D. M. Briercheck. 1994. Infrared spectroscopic detection of light-induced change in chloride-arginine interaction in halorhodopsin. *Biochemistry.* 33:1629–1635.

Casadio, R., H. Gutowitz, P. C. Mowery, M. Taylor, and W. Stoeckenius. 1980. Light-dark adaptation of bacteriorhodopsin in Triton-treated purple membrane. *Biochim. Biophys. Acta.* 590:13–23.

Dencher, N. A., C. N. Rafferty, and W. Sperling. 1976. 13-*cis* and *trans* bacteriorhodopsin: photochemistry and dark equilibrium. *Ber. Kernforschungsanlage Juelich.* 1347:1–42.

Diller, R., M. Stockburger, D. Oesterhelt, and J. Tittor. 1987. Resonance Raman study of intermediates of the halorhodopsin photocycle. *FEBS Lett.* 217:297–304.

Duschl, A., J. K. Lanyi, and L. Zimányi. 1990. Properties and photochemistry of a halorhodopsin from the haloalkalophile, *Natronobacterium pharaonis*. *J. Biol. Chem.* 265:1261–1267.

Duschl, A., M. A. McCloskey, and J. K. Lanyi. 1988. Reconstitution of halorhodopsin: properties of halorhodopsin-containing proteoliposomes. *J. Biol. Chem.* 263:17016–17022.

Fahr, A., and E. Bamberg. 1982. Photocurrents of dark-adapted bacteriorhodopsin on black lipid membranes. *FEBS Lett.* 140:251–253.

Falke, J. J., S. I. Chan, M. Steiner, D. Oesterhelt, P. Towner, and J. K. Lanyi. 1984. Halide binding by the purified halorhodopsin chromoprotein. II. New chloride binding sites revealed by ^{35}Cl NMR. *J. Biol. Chem.* 259: 2185–2189.

Fodor, S. P., R. A. Bogomolni, and R. A. Mathies. 1987. Structure of the retinal chromophore in the hR_L intermediate of halorhodopsin from resonance Raman spectroscopy. *Biochemistry.* 26:6775–6778.

Gergely, C., C. Ganea, and G. Váró. 1994. Combined optical and photoelectric study of the photocycle of 13-*cis* bacteriorhodopsin. *Biophys. J.* 67:855–861.

Golub, G., and W. Kahan. 1995. Calculating the singular values and pseudo-inverse of a matrix. *SIAM J. Num. Anal.* 2:205–224.

Harbison, G. S., S. O. Smith, J. A. Pardoen, C. Winkel, J. Lugtenburg, J. Herzfeld, R. A. Mathies, and R. G. Griffin. 1984. Dark-adapted bacteriorhodopsin contains 13-*cis*, 15-*syn* and all-*trans*, 15-*anti* retinal Schiff bases. *Proc. Natl. Acad. Sci. USA.* 81:1706–1709.

Havelka, W. A., R. Henderson, J. A. W. Heymann, and D. Oesterhelt. 1993. Projection structure of halorhodopsin from *Halobacterium halobium* at 6 Å resolution obtained by electron cryo-microscopy. *J. Mol. Biol.* 234: 837–846.

Hazemoto, N., N. Kamo, Y. Terayama, Y. Kobatake, and M. Tsuda. 1983. Photochemistry of two rhodopsinlike pigments in bacteriorhodopsin-free mutant of *Halobacterium halobium*. *Biophys. J.* 44:59–64.

Hazemoto, N., N. Kamo, and Y. Kobatake. 1984. Suggestion of existence of two forms of halorhodopsin in alkaline solution. *Biochem. Biophys. Res. Commun.* 118:502–507.

Hegemann, P., D. Oesterhelt, and M. Steiner. 1985. The photocycle of the chloride pump halorhodopsin. I. Azide catalyzed deprotonation of the chromophore is a side reaction of photocycle intermediates inactivating the pump. *EMBO J.* 4:2347–2350.

Hofrichter, J., E. R. Henry, and R. H. Lozier. 1989. Photocycles of bacteriorhodopsin in light- and dark-adapted purple membrane studied by time-resolved absorption spectroscopy. *Biophys. J.* 56:693–706.

Kalisky, O., C. R. Goldschmidt and M. Ottolenghi. 1977. On the photocycle and light adaptation of dark-adapted bacteriorhodopsin. *Biophys. J.* 19: 185–189.

Kamo, N., N. Hazemoto, Y. Kobatake, and Y. Mukohata. 1985. Light and dark adaptation of halorhodopsin. *Arch. Biochem. Biophys.* 238:90–96.

Kataoka, M., H. Kamikubo, F. Tokunaga, L. S. Brown, Y. Yamazaki, A. Maeda, M. Sheves, R. Needleman, and J. K. Lanyi. 1994. Energy coupling in an ion pump: the reprotonation switch of bacteriorhodopsin. *J. Mol. Biol.* 243:621–638.

Kobayashi, T., H. Ohtani, J.-I. Iwai, A. Ikegami, and H. Uchiki. 1983. Effect of pH on the photoreaction cycles of bacteriorhodopsin. *FEBS Lett.* 162: 197–200.

Lanyi, J. K. 1984. Light-dependent *trans* to *cis* isomerization of the retinal in halorhodopsin. *FEBS Lett.* 175:337–342.

Lanyi, J. K. 1986a. Photochromism of halorhodopsin: *cis/trans* isomerization of the retinal around the 13–14 double bond. *J. Biol. Chem.* 261: 14025–14030.

Lanyi, J. K. 1986b. Halorhodopsin: a light-driven chloride pump. *Annu. Rev. Biophys. Biophys. Chem.* 15:11–28.

Lanyi, J. K. 1990. Halorhodopsin: a light-driven electrogenic chloride transport system. *Physiol. Rev.* 70:319–330.

Lanyi, J. K. 1992. Proton transfer and energy coupling in the bacteriorhodopsin photocycle. *J. Bioenerg. Biomembr.* 24:169–179.

Lanyi, J. K. 1993. Proton translocation mechanism and energetics in the light-driven pump bacteriorhodopsin. *Biochim. Biophys. Acta Bioenerg.* 1183:241–261.

Lanyi, J. K., A. Duschl, G. W. Hatfield, K. M. May, and D. Oesterhelt. 1990a. The primary structure of a halorhodopsin from *Natronobacterium pharaonis*: structural, functional and evolutionary implications for bacterial rhodopsins and halorhodopsins. *J. Biol. Chem.* 265:1253–1260.

Lanyi, J. K., A. Duschl, G. Váró, and L. Zimányi. 1990b. Anion binding to the chloride pump, halorhodopsin, and its implications for the transport mechanism. *FEBS Lett.* 265:1–6.

Lanyi, J. K., and B. Schobert. 1983. Effects of chloride and pH on the chromophore and photocycling of halorhodopsin. *Biochemistry.* 22:2763–2769.

Lanyi, J. K., and V. Vodyanoy. 1986. Flash spectroscopic studies of the kinetics of the halorhodopsin photocycle. *Biochemistry.* 25:1465–1470.

Lozier, R. H., W. Niederberger, M. Ottolenghi, G. Sivorinovsky, and W. Stoeckenius. 1978. On the photocycles of light- and dark-adapted bacteriorhodopsin. *In Energetics and Structure of Halophilic Microorganisms.* S. R. Caplan, and M. Ginzburg, editors. Elsevier/North Holland, Amsterdam. 123–139.

Maeda, A., T. Ogurusu, T. Yoshizawa, and T. Kitagawa. 1985. Resonance Raman study on binding of chloride to the chromophore of halorhodopsin. *Biochemistry.* 24:2517–2521.

Mowery, P. C., R. H. Lozier, Q. Chae, Y. W. Tseng, M. Taylor, and W. Stoeckenius. 1979. Effect of acid pH on the absorption spectra and photoreactions of bacteriorhodopsin. *Biochemistry.* 18:4100–4107.

Needleman, R., M. Chang, B. Ni, G. Váró, J. Fornes, S. H. White, and J. K. Lanyi. 1991. Properties of asp212-asn bacteriorhodopsin suggest that asp212 and asp85 both participate in a counterion and proton acceptor complex near the Schiff base. *J. Biol. Chem.* 266:11478–11484.

Oesterhelt, D., P. Hegemann, P. Tavan, and K. Schulten. 1986. *Trans-cis* isomerization of retinal and a mechanism for ion translocation in halorhodopsin. *Eur. Biophys. J.* 14:123–129.

Oesterhelt, D., P. Hegemann, and J. Tittor. 1985. The photocycle of the chloride pump halorhodopsin. II. Quantum yields and a kinetic model. *EMBO J.* 4:2351–2356.

Oesterhelt, D., and W. Stoeckenius. 1974. Isolation of the cell membrane of *Halobacterium halobium* and its fractionation into red and purple membrane. *Methods Enzymol.* 31:667–678.

Oesterhelt, D., J. Tittor, and E. Bamberg. 1992. A unifying concept for ion translocation by retinal proteins. *J. Bioenerg. Biomembr.* 24:181–191.

Ogurusu, T., A. Maeda, N. Sasaki, and T. Yoshizawa. 1982. Effects of chloride on the absorption spectrum and photoreactions of halorhodopsin. *Biochim. Biophys. Acta.* 682:446–451.

Ogurusu, T., A. Maeda, and T. Yoshizawa. 1984. Absorption spectral properties of purified halorhodopsin. *J. Biochem.* 95:1073–1082.

Otomo, J., H. Tomioka, and H. Sasabe. 1992. Properties and the primary structure of a new halorhodopsin from halobacterial strain mex. *Biochim. Biophys. Acta Biomembr.* 1112:7–13.

Otto, H., T. Marti, M. Holz, T. Mogi, L. J. Stern, F. Engel, H. G. Khorana, and M. P. Heyn. 1990. Substitution of amino acids Asp-85, Asp-212, and Arg-82 in bacteriorhodopsin affects the proton release phase of the pump and the pK of the Schiff base. *Proc. Natl. Acad. Sci. USA.* 87:1018–1022.

Pande, C., J. K. Lanyi, and R. H. Callender. 1989. Effects of various anions on the Raman spectrum of halorhodopsin. *Biophys. J.* 55:425–431.

Rothschild, K. J., O. Bousche, M. S. Braiman, C. A. Hasselbacher, and J. L. Spudich. 1988. Fourier transform infrared study of the halorhodopsin chloride pump. *Biochemistry.* 27:2420–2424.

Scharf, B., and M. Engelhard. 1994. Blue halorhodopsin from *Natronobacterium pharaonis*: wavelength regulation by anions. *Biochemistry.* 33: 6387–6393.

Schobert, B., and J. K. Lanyi. 1982. Halorhodopsin is a light-driven chloride pump. *J. Biol. Chem.* 257:10306–10313.

Schobert, B., and J. K. Lanyi. 1986. Electrostatic interaction between anions bound to site I and the Schiff-base of halorhodopsin. *Biochemistry.* 25: 4163–4167.

Schobert, B., J. K. Lanyi, and E. J. J. Cragoe. 1983. Evidence for a halide binding site in halorhodopsin. *J. Biol. Chem.* 258:15158–15164.

Schobert, B., J. K. Lanyi, and D. Oesterhelt. 1986. Effects of anion binding on the deprotonation reactions of halorhodopsin. *J. Biol. Chem.* 261: 2690–2696.

Shichida, Y., S. Matuoka, Y. Hidaka, and T. Yoshizawa. 1983. Absorption spectra of intermediates of bacteriorhodopsin measured by laser photolysis at room temperatures. *Biochim. Biophys. Acta.* 723:240–246.

Spencer, D. B., and T. G. Dewey. 1990. Activation parameters for the halorhodopsin photocycle: a phase lifetime spectroscopic study of the 520- and 640-nanometer intermediates. *Biochemistry.* 29:3140–3145.

Steiner, M., D. Oesterhelt, M. Ariki, and J. K. Lanyi. 1984. Halide binding by the purified halorhodopsin chromoprotein. I. Effects on the chromophore. *J. Biol. Chem.* 259:2179–2184.

Stern, L. J., P. L. Ahl, T. Marti, T. Mogi, M. Duñach, S. Berkovitz, K. J. Rothschild, and H. G. Khorana. 1989. Substitution of membrane-embedded aspartic acids in bacteriorhodopsin causes specific changes in different steps of the photochemical cycle. *Biochemistry.* 28:10035–10042.

Thorgeirsson, T. E., S. J. Milder, L. J. W. Miercke, M. C. Betlach, R. F. Shand, R. M. Stroud, and D. S. Kliger. 1991. Effects of Asp-96→Asn, Asp-85→Asn, and Arg-82→Gln single-site substitutions on the photocycle of bacteriorhodopsin. *Biochemistry.* 30:9133–9142.

Tittor, J., D. Oesterhelt, R. Maurer, H. Desel, and R. Uhl. 1987. The photochemical cycle of halorhodopsin: absolute spectra of intermediates obtained by flash photolysis and fast difference spectra measurements. *Biophys. J.* 52:999–1006.

Tsuda, M., N. Hazemoto, M. Kondo, N. Kamo, Y. Kobatake, and Y. Terayama. 1982. Two photocycles in *Halobacterium halobium* that lacks bacteriorhodopsin. *Biochem. Biophys. Res. Commun.* 108:970–976.

Váró, G., and J. K. Lanyi. 1989. Photoreactions of bacteriorhodopsin at acid pH. *Biophys. J.* 56:1143–1151.

Váró, G., and J. K. Lanyi. 1991a. Kinetic and spectroscopic evidence for an irreversible step between deprotonation and reprotonation of the Schiff base in the bacteriorhodopsin photocycle. *Biochemistry.* 30:5008–5015.

Váró, G., and J. K. Lanyi. 1991b. Thermodynamics and energy coupling in the bacteriorhodopsin photocycle. *Biochemistry.* 30:5016–5022.

Walter, T. J., and M. S. Braiman. 1994. Anion-protein interactions during halorhodopsin pumping: halide binding at the protonated Schiff base. *Biochemistry.* 33:1724–1733.

Zimányi, L., Y. Cao, M. Chang, B. Ni, R. Needleman, and J. K. Lanyi. 1992. The two consecutive M substates in the photocycle of bacteriorhodopsin are affected specifically by the D85N and D96N residue replacements. *Photochem. Photobiol.* 56:1049–1055.

Zimányi, L., L. Keszthelyi, and J. K. Lanyi. 1989a. Transient spectroscopy of bacterial rhodopsins with optical multichannel analyser. I. Comparison of the photocycles of bacteriorhodopsin and halorhodopsin. *Biochemistry.* 28:5165–5172.

Zimányi, L., and J. K. Lanyi. 1987. Iso-halorhodopsin: a stable 9-*cis* retinal-containing photoproduct of halorhodopsin. *Biophys. J.* 52:1007–1013.

Zimányi, L., and J. K. Lanyi. 1989a. Transient spectroscopy of bacterial rhodopsins with optical multichannel analyzer. II. Effects of anions on the halorhodopsin photocycle. *Biochemistry.* 28:5172–5178.

Zimányi, L., and J. K. Lanyi. 1989b. Low temperature photoreactions of halorhodopsin. II. Description of the photocycle and its intermediates. *Biochemistry.* 28:1662–1666.

Zimányi, L., and J. K. Lanyi. 1993. Deriving the intermediate spectra and photocycle kinetics from time-resolved difference spectra of bacteriorhodopsin: the simpler case of the recombinant D96N protein. *Biophys. J.* 64:240–251.

Zimányi, L., P. Ormos, and J. K. Lanyi. 1989b. Low temperature photoreactions of halorhodopsin. I. Detection of conformational substates of the chromophore. *Biochemistry.* 28:1656–1661.